



CrossMark  
click for updates

Cite this: DOI: 10.1039/c5sm01824b

# Efficient nematode swimming in a shear thinning colloidal suspension†

Jin-Sung Park,<sup>‡,ab</sup> Daeyeon Kim,<sup>‡,a</sup> Jennifer H. Shin<sup>a</sup> and David A. Weitz<sup>\*,b</sup>

The swimming behavior of a nematode *Caenorhabditis elegans* (*C. elegans*) is investigated in a non-Newtonian shear thinning colloidal suspension. At the onset value ( $\phi \sim 8\%$ ), the suspension begins to exhibit shear thinning behavior, and the average swimming speed of worms jumps by approximately 12% more than that measured in a Newtonian solution exhibiting no shear dependent viscosity. In the shear thinning regime, we observe a gradual yet significant improvement in swimming efficiency with an increase in  $\phi$  while the swimming speed remains nearly constant. We postulate that this enhanced swimming can be explained by the temporal change in the stroke form of the nematode that is uniquely observed in a shear thinning colloidal suspension: the nematode features a fast and large stroke in its head to overcome the temporally high drag imposed by the viscous medium, whose effective viscosity ( $\eta_s$ ) is shown to drop drastically, inversely proportional to the strength of its stroke. Our results suggest new insights into how nematodes efficiently maneuver through the complex fluid environment in their natural habitat.

Received 23rd July 2015,  
Accepted 7th December 2015

DOI: 10.1039/c5sm01824b

[www.rsc.org/softmatter](http://www.rsc.org/softmatter)

## 1. Introduction

Undulatory organismal locomotion is widely observed in nature and ranges from the beating of spermatozoa flagellum or intestinal parasites to the crawling of nematodes or snakes.<sup>1–8</sup> These organisms commonly generate propulsive force by pushing their bodies laterally against the surrounding terrestrial environment utilizing sinusoidal waves that propagate along their slender bodies.<sup>9</sup> Recent experimental observations revealed that the physical properties of the environments such as viscosity, elasticity, granularity, and geometry can lead to changes in the locomotory behavior of these organisms.<sup>10–14</sup> For example, the studies on the swimming behavior of spermatozoa have demonstrated marked alterations in the stroke patterns of their flagella into hyperactive forms in fluids of increased viscosity.<sup>15,16</sup> Furthermore, the sandfish lizard was shown to move effectively in the medium consisting of dense granular particles by changing its locomotion gate to the undulatory swimming mode in order to generate thrust to overcome high drag.<sup>17,18</sup>

A series of recent theoretical and experimental studies addressed how the elasticity of complex fluids could alter the dynamics and kinematics of micro-swimmers.<sup>19–27</sup> According to these results, the fluid elasticity can either enhance or retard the swimming depending on the stroke form of the swimmers and the properties of working fluids. One of the marked characteristic properties of complex fluids is the phenomenon of shear-dependent viscosity, in which the fluid viscosity changes with the applied shear rate. Because most undulatory organisms gain thrust by applying shear to the surrounding complex medium using their unique stroke motion, it is crucial to understand how the inherent properties of complex fluids play a role in the motility of the undulatory swimmers in such environments.<sup>28–31</sup>

In this paper, we investigate the effect of shear thinning viscosity on the swimming locomotion of *C. elegans* whose natural environment is known as wet soil, the particulate system exhibiting a typical shear thinning viscosity.<sup>10,11</sup> Previously, in a viscoelastic carboxymethyl cellulose (CMC) solution with no significant shear thinning viscosity, the swimming speed of nematodes was shown to be slower than that measured in a purely viscous fluid.<sup>32</sup> In a shear thinning xanthan gum (XG) polymeric solution, on the other hand, the nematode's swimming speed was shown to remain relatively constant in semi-dilute regimes where the shear rate dependence of the viscosity is low.<sup>33</sup> On the contrary, here we report that the enhanced swimming speed of *C. elegans* in a shear thinning polystyrene (PS) colloidal suspension, which is accompanied by marked alterations in the stroke form. Unlike the XG polymeric solution, the PS colloidal

<sup>a</sup> School of Mechanical, Aerospace and Systems Engineering, Division of Mechanical Engineering, Korea Advanced Institute of Science and Technology, Daejeon 305-701, Republic of Korea

<sup>b</sup> School of Engineering and Applied Sciences and Department of Physics, Harvard University, Cambridge, Massachusetts 02138, USA.  
E-mail: [weitz@seas.harvard.edu](mailto:weitz@seas.harvard.edu)

† Electronic supplementary information (ESI) available: Movies of swimming nematodes in a MC solution (Movie S1.avi) and colloidal suspension (Movie S2.avi). See DOI: 10.1039/c5sm01824b

‡ These authors contributed equally to this work.

suspension features a steep drop of  $\eta_s$ , exhibiting dual characteristics of both the shear thinning and Newtonian behavior over the range of shear rate relevant to the swimming nematodes. We postulate that this enhanced swimming is related to the hyper-stroke motion of *C. elegans* and a large local shear gradient of the shear thinning colloidal solutions, which result in reduction of effective viscosity that oppose the motion during their undulating cycle. Our paper is the first experimental evidence that illustrates how the shear thinning property of colloidal suspensions can induce the change in stroke form of the swimming nematode, leading to the swimming enhancement.

## 2. Experimental section

### 2.1. Materials and sample preparation

A wild type (N2) strain of *C. elegans* was purchased from *Caenorhabditis* genetic center (University of Minnesota, Minneapolis). After cultivating them on the lawn of OP50 bacteria grown on the NGM agar plate (1.7% Bacto agar, 2.5 g Bacto peptone, 3 g NaCl, 1 ml 1 M CaCl<sub>2</sub>, 1 ml 1 M MgSO<sub>4</sub>, 25 ml 1 M potassium phosphate buffer, and 1 ml 5  $\mu\text{g mL}^{-1}$  cholesterol to 975 ml water) at room temperature, the nematodes in the stage of young adults (body length  $\sim 1000\ \mu\text{m}$ , body thickness  $\sim 60\ \mu\text{m}$ ) were selected for experiments.<sup>34</sup>

To avoid any disruption in rheological property of colloidal suspension by screening of salt ions dissolved in a buffer solution, all experiments presented here were only conducted in distilled water. Colloidal suspensions were prepared by mixing mono-disperse PS particles (600 nm diameter) in DI water at six different volume fractions ( $\phi = 1.6, 4, 8, 12, 16$ , and  $22\%$ ). Methylcellulose (MC) solutions (molecular weight  $\sim 63\ 000$  Da, Sigma Aldrich, M0387), known as typical viscoelastic fluids, do not exhibit shear rate dependence in the low-intermediate range of the shear rate, having relatively constant  $\eta_s$  values over the measured range of the shear rates ( $1\text{--}100\ \text{s}^{-1}$ ), although the absolute viscosity values of the solutions are much higher than those of water [black circles in Fig. 1(A) and (B)].

### 2.2. Rheology measurement

To characterize the fluid rheological properties, we measured the shear viscosity ( $\eta_s$ ) using a double-gap couette plate (cylinder volume: 9 ml) of a TA Ares G2, strain-controlled rheometer. Next, we measured the rheological properties of PS colloidal suspensions for six different  $\phi$  (Fig. 1(B)). At the low  $\phi$  concentrations of 1.6 and 4%, the PS suspensions behaved similarly to simple Newtonian fluids, and the estimated  $\eta_s$  was similar to that of DI water. The shear thinning phenomenon begins to appear from  $\phi \sim 8\%$ . Also, there exists a transition point where the fluid exhibits a transient Newtonian-like behavior following a rapid drop in  $\eta_s$  [solid line in Fig. 1(B)]. This rheological transition is a generic characteristics of particulated fluids due to the rearrangements of particles by shearing flow,<sup>35,36</sup> which differentiates the PS colloidal suspensions from the XG

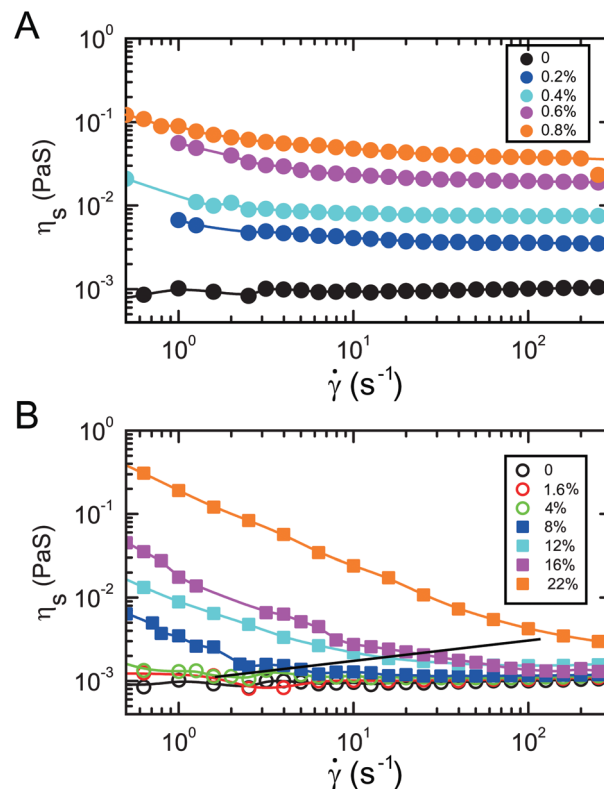


Fig. 1 Shear viscosity as a function of shear rate measured at methylcellulose (MC) solutions at four different concentrations (0.2, 0.4, 0.6, and 0.8 wt%) (A) and six different concentrations of polystyrene (PS) colloidal suspensions ( $\phi = 1.6, 4, 8, 12, 16$ , and  $22\%$ ) (B). Here, the solid line in (B) indicates the transition points to Newtonian-like fluids from the shear thinning fluids. In (A) and (B), black circles are the plots for distilled water.

polymeric solutions whose viscosity decreases monotonically with shear rate.<sup>33</sup>

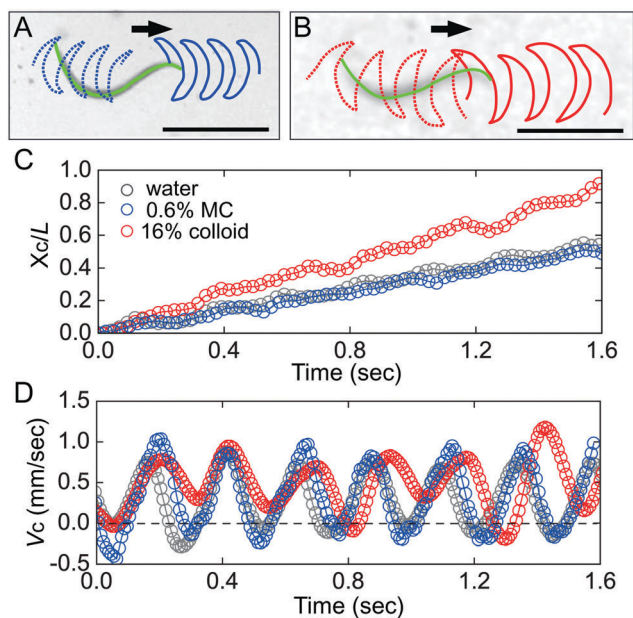
The maximum value in the instantaneous head velocity of swimming nematodes is about  $4\ \text{mm s}^{-1}$  (Fig. 4(D)). Thus, the range of shear rates that could be applied to fluid by propagation of a nematode,  $\dot{\gamma} = v/r$ , can reach up to  $\sim 130\ \text{s}^{-1}$  where  $v$  is the maximum stroke velocity at the nematode's head and  $r$  is the radius of the nematode's body. In such a range of shear rates, the nematode would experience a larger variation in  $\eta_s$ , by over one order of magnitude in each undulating cycle. However, the fluid viscosities of PS suspensions with  $\phi = 8, 12$ , and  $16\%$  at low shear regimes are similar to those of 0.2, 0.4, and  $0.6\%$  MC solutions, respectively.

### 2.3. Experimental observation

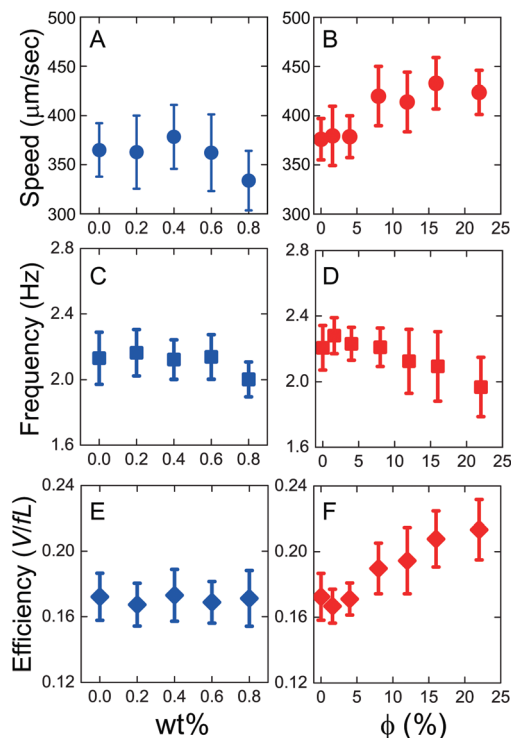
The experimental observations were performed in a shallow slide glass chamber with a height of  $120\ \mu\text{m}$  (chamber dimension:  $5 \times 1.5\ \text{cm}^2$ ). The nematodes were then transferred into colloidal suspensions of different  $\phi$ , and the mixtures were gently injected into the chamber. A digital video camera (HDR-HC9, Sony) mounted on a stereo-microscope (SMZ 800, Nikon) was used to record swimming nematodes at 30 Hz, and a high speed camera was used for detailed analysis of the high stroke nematode's motions at 120 Hz.

### 3. Results and discussion

Snapshot images of representative nematodes swimming in the 0.6% MC solution and 16% colloidal suspension are shown in Fig. 2(A) and (B), respectively. The trajectories of heads (solid lines) and tails (dotted lines) of the nematodes were taken from two end points of the schematic skeletons drawn along the body center (green lines) for  $\Delta t = 1.6$  s, and the moving displacements were normalized to the nematode body lengths as shown in Fig. 2(C). Here,  $X_c$  is the position of the  $x$ -component in the center of mass obtained from the schematic skeletons. The measured swimming speeds of the nematodes were each  $360$  and  $440 \mu\text{m s}^{-1}$  in the 0.6% MC solution (blue circles) and 16% colloidal suspension (red circles), respectively. While the nematode swimming speed in 0.6% MC solution was almost same to that measured in DI water (gray circles), it was increased approximately 22% in 16% colloidal suspension. Interestingly, like in the previous numerical results on a finite sheet,<sup>37</sup> we also found that nematodes exhibit oscillatory movement in a backward and forward step for each cycle in both water and 16% colloid suspension although their net displacement per one stroke cycle propagates forward as shown in Fig. 2(C). However, the backward movement of nematodes, indicated by negative speed values below the dotted line in



**Fig. 2** The swimming motion of nematodes observed in two different fluids: trajectories of nematodes in 0.6% MC solution (A) and 16% colloidal suspension (B) are drawn at each heads (solid lines) and tails (dotted lines) of nematode's skeletons (green lines) drawn along the body center (total recording duration:  $\Delta t = 1.6$  s). The arrow in (A) indicates the swimming direction of a nematode. The locations of the  $x$ -component of swimming nematodes (C) and the velocity profiles in  $x$  direction (D) are calculated from the nematode's center of mass in MC solution (blue circles) and colloidal suspension (red circles). For comparison, the moving displacement and the velocity profile measured in DI water (gray circles) are drawn in (C) and (D), respectively. The horizontal dotted line in graph (D) is marked the "0" velocity line and the scale bars in (A) and (B) are  $500 \mu\text{m}$ . See ESI MovieS1.avi and MovieS2.avi† for corresponding movies.



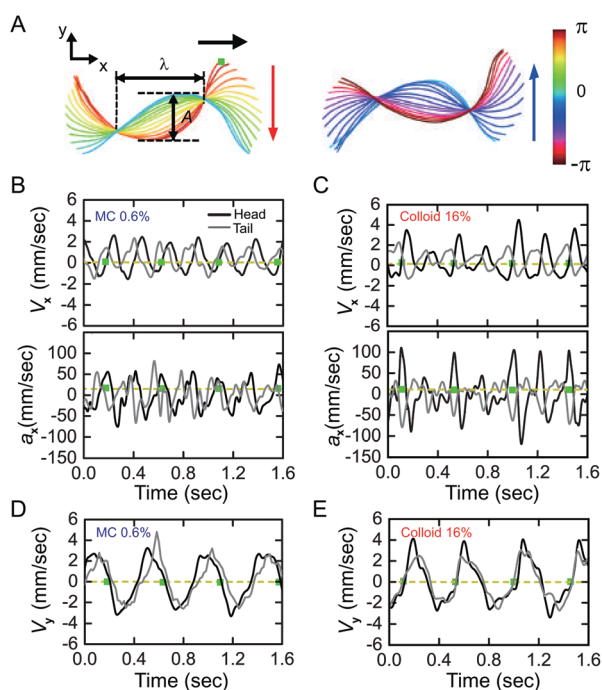
**Fig. 3** Swimming behaviors of nematodes observed in two different fluids: swimming speed (A), undulating frequency (C), and motion efficiency (E) measured from methylcellulose (MC) solutions with four different polymer concentrations (0.2, 0.4, 0.6, and 0.8 wt%). While (B), (D), and (F) were the values measured from six different colloidal suspensions ( $\phi = 1.6, 4, 8, 12, 16$ , and  $22\%$ ) and distilled water. Compared to ones from the MC solution ((A) and (E)), the measured swimming speed (B) and efficiency (F) in colloidal suspensions is both increased. Here, an average over 10 nematodes are recorded for each experiment and the error bars are standard deviation.

Fig. 2(D), is noticeably decreased when they swim in colloidal suspensions, thereby leading to enhanced forward movement for nematodes.

Fig. 3 illustrates the differential swimming behavior of nematodes observed in the Newtonian MC solutions (blue) and non-Newtonian PS colloidal suspensions (red). In 0–0.6% weight fractions of MC solutions, the measured swimming speeds ( $V$ ) and undulatory frequencies ( $f$ ) of nematodes remain statistically the same as those measured in water ( $\bar{v} = 376 \pm 21 \mu\text{m s}^{-1}$  and  $\bar{f} = 2.12 \pm 0.16 \text{ Hz}$ ) with a slight decrease in the 0.8 wt% solution (Fig. 3(A) and (C)). The ratio of swimming speed to characteristic speed, a product of the nematode undulatory frequency and body length ( $V/fL$ ), can be considered a dimensionless quantity showing the undulating efficiency of the swimmer's motion.<sup>8,18</sup> This value was found to remain constant over the entire tested range of the viscosities in the MC solutions (Fig. 3(E)). Our measurements in the MC solutions are in agreement with previous findings in the similarly viscous CMC solution.<sup>32,38</sup> This viscosity-independent swimming behavior of a nematodes is likely due to the fact that the mean power of nematodes is also increased with the viscosity of fluids.<sup>39–41</sup>

In contrast, the swimming of nematodes in colloidal suspensions exhibited a noticeable enhancement at the onset of shear thinning characteristics in the PS solution ( $\phi = 8\%$ ) (Fig. 3(B)). At  $\phi = 8\%$ , the averaged speed was approximately 12% faster ( $\bar{v} = 420 \pm 30 \mu\text{m s}^{-1}$ ) than that measured in water and MC solutions. With a further increase in  $\phi$ , the swimming speed of nematodes remained constant ( $\phi = 12, 16$ , and  $22\%$  in Fig. 3(B)). By contrast, the undulatory frequency of nematodes ( $f$ ) exhibited a gradual decrease from  $2.20 \pm 0.11 \text{ Hz}$  ( $\phi = 8\%$ ) to  $1.96 \pm 0.18 \text{ Hz}$  ( $\phi = 22\%$ ) in the shear thinning fluids (Fig. 3(D)). As a result, the swimmer motion efficiency ( $V/fL$ ) in colloidal suspensions showed significant enhancement with  $\phi$  (Fig. 3(F)).

We next address the question of how the shear thinning viscosity correlates with the enhanced swimming efficiency of nematodes. Fig. 4(A) shows the color-coded temporal evolution of nematode skeletons over each half oscillating cycle in 0.6% MC solution. The nematode's stroke ratio of undulating amplitude ( $A$ ) to wavelength ( $\lambda$ ) increased from 0.528 (MC solution) to 0.607 (PS suspension) in the downward oscillating phase [left in Fig. 4(A)] and from 0.438 (MC solution) to 0.537 (PS suspension) in the upward oscillating phase [right in Fig. 4(A)].



**Fig. 4** The stroke behaviors of swimming nematodes observed in two different fluids: overlapped images of skeletons show the stroke shapes over each half oscillating cycles in the 0.6% MC solution. Here, the red and blue arrow in (A) indicates the oscillating direction during stroke cycles. The wavelength ( $\lambda$ ) and amplitude ( $A$ ) of the undulating nematode is defined from two node points as drawn in (A). The tangential ( $V_x$ ) and normal velocities ( $V_y$ ) in the stroke motions of nematodes are taken from each heads (black lines) and tails (gray lines) of skeletons [(B) and (D): MC solution, and (C) and (E): colloidal suspension]. The below graphs in (B) and (C) show the acceleration for the tangential ( $V_x$ ) from each heads and tails of skeletons. Here, the locations of “ $\pi$ ” phase states (rectangular symbol in (A)) during their stroke cycles are each marked in the graph (B)–(E).

Next, in Fig. 4(B)–(E), we showed the longitudinal ( $V_x$ ) and lateral ( $V_y$ ) components of the stroke velocity from the stroke trajectories of the head (black line) and tail (gray line) of the nematodes by tracking both ends of nematode skeletons. Here, we noted a few remarkable differences in the stroke patterns in the PS colloidal suspension compared to those in the MC solution.

First of all, the amplitude of the  $V_x$  oscillation in the PS colloidal suspension at the head (black line in the upper graph of Fig. 4(C)) becomes twice as large as that measured in MC solution (black line in the upper graph of Fig. 4(B)). In other words, the  $V_x$  graph gets shifted upward with a bias for the forward motion in PS colloid suspensions, resulting in faster propulsion than what would be expected in the MC solution. Similarly, the time rate change in the oscillating velocity ( $a_x$ ), which may be related to the muscular force, is higher in the colloidal suspension (black line in the lower graph of Fig. 4(C)) than that for the MC solution (black line in the lower graph of Fig. 4(B)). Now, let us suppose that a drastic drop in  $\eta_s$  in a shear thinning fluid causes a large variation in undulating velocity. When nematodes are fully contracted in a 16% colloidal suspension [“ $\pi$ ” phase state in Fig. 4(A)], they would feel a much larger  $\eta_s$  from the PS colloidal suspension because its instantaneous undulating velocity is almost “0”. To overcome such a high drag, which is about one hundred times more than that of water, nematodes would have to increase their muscular power as previously reported.<sup>40,41</sup> As a result, the generated high stroke power consequently imposes higher rate of shearing in the PS colloidal suspension, resulting in a drastic drop in the apparent viscosity of the medium,  $\eta_s$ . Interestingly, we note that the amplitude of  $V_x$  alternates between two amplitudes at the nematode's head in a 16% PS colloidal suspension (black line in the upper graph of Fig. 4(C)). This alternative oscillation is more pronounced in the time rate change ( $a_x$ ) of the longitudinal component ( $V_x$ ) (black line in the lower graph of Fig. 4(C)). We hypothesize that this alternative oscillation is mediated by unequal ventral/dorsal bending force due to the asymmetry in the ventral/dorsal neurological (or physiological) structure, evidenced by the recent experimental results.<sup>38,42</sup>

The powerful stroke of the nematodes in PS colloidal suspension was also reflected in the analysis of bending angle ( $\theta$ ), calculated from the time-variation of local curvature at both end points of the nematode's skeletons (red line in Fig. 5(A)) during their periodic oscillations. Here, the averaged value of maximum bending angle ( $\theta_M$ ) measured at every “ $\pm\pi$ ” phase states was larger in 16% colloidal suspension than in 0.6% MC solution whereas in the tail,  $\theta_M$  was rather decreased in the colloidal suspension because the muscular power was shown to gradually attenuate from the nematode's head to the tail as the wave propagates along its body, resulting in a decrease in the amplitude of the tail stroke.

The alteration in the stroke form of the nematode might be crucial for understanding the mechanism of its enhanced swimming. As illustrated previously in the other experiments, the self-propulsive micro-swimmer is principally considered to a force-free swimmer in which a fluid drag simultaneously

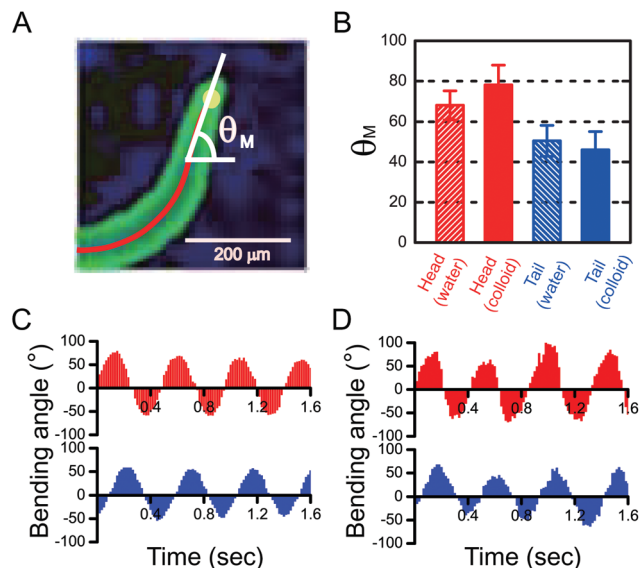


Fig. 5 The analysis of bending angles of nematodes swimming in two different fluids: pseudo-color image of nematode swimming in 16% colloidal suspension (A), and statistical analysis for maximum bending angle ( $\theta_M$ ) measured at each head and tail points of nematodes in the MC solution and colloidal suspension (B). The continuous change in bending angle of swimming nematodes [0.6% MC solution (C) and 16% colloidal suspension (D)] is measured during 1.6 s. Here, the position of bending angle is measured at the end points (yellow circle) of skeleton line (red in (A)).

resists and generates its forward motion.<sup>3</sup> Thus, the fluid viscosity is irrelevant to propulsion speed of a swimmer as far as its stroke form is held constant. For example, over a broad range of semi-dilute solutions of XG polymers with a moderate shear gradient, the nematodes exhibited no significant changes in their swimming speed or stroke forms.<sup>33</sup> While their observations seem contradicting our experimental findings, one must note that the XG solutions made of semi-dilute rod-shape polymers used by Gagnon *et al.*<sup>33</sup> are very different from the PS colloidal suspensions used in our experiments.

Compared to the semi-dilute XG polymeric solution, the drop in  $\eta_s$  is steeper in the PS colloidal suspensions over the shear range of 0–130  $s^{-1}$ , relevant to the stroke rate of swimming *C. elegans*. As a result, the swimming *C. elegans* would experience much larger difference in  $\Delta\eta$  during the one stroke cycle in PS colloidal suspensions than in the semi-dilute XG polymeric solutions. More importantly, there exists the transition point in PS colloidal suspensions where  $\eta$  shows Newtonian-like behavior. When *C. elegans* swims in shear thinning colloidal suspension, the nematodes would work against the dramatically varying load of shear thinning viscosity by adaptively altering their stroke and move forward fast by shearing against the fluid in the water-like regime of low viscosity with constant  $\eta$  values. Therefore, it seems plausible to postulate that the alterations in the stroke form would be critical in the enhancement of the swimming speed as well as the shear thinning effect of the surrounding medium.

Recently, Man and Lauga<sup>43</sup> showed that the alteration in the micro-rheological property near the surface of a swimmer may

lead to the enhancement in the swimming speed. This theory was based on the well-known phenomenon of phase slip where the micro-structured fluids would phase-separate near the surface to the low-viscosity layer. In fact, Man and Lauga described the speed enhancement of *C. elegans* in XG solution made of  $\sim 200$   $\mu m$  diameter polymers where the thickness of the viscous depletion layer was 40–120  $\mu m$ . If the proposed theoretical model were also true for our PS colloidal system, the swimming enhancement of *C. elegans* would have increased dramatically, possibly by orders of magnitude because the wall depletion layer in a PS colloidal suspension (diameter of particle  $\sim 600$  nm) would be only of the order of 1  $\mu m$ .<sup>43,44</sup>

Taken all together, a drastic drop of  $\eta_s$  in a PS colloidal suspension could alter the kinematics of a nematode which is closely related with the adaptive variations in its neuromuscular power. Indeed, it was previously reported that the increase in a fluid viscosity could induce the increase in Young's modulus and effective tissue viscosity of the nematode's body to overcome an increased fluid drag force, but in the limit of its finite power output.<sup>39–41</sup>

## 4. Conclusions

In conclusion, we report a significant enhancement in a nematode's swimming speed and efficiency in a non-Newtonian colloidal suspension where the effective thinning of apparent viscosity induced by the nematodes fast and powerful stroke motion plays a critical role. Given the recent experimental results illustrating how a shear thinning XG polymeric solution does not alter the nematodes swimming kinematics,<sup>33</sup> our study emphasizes the fact that rheological differences among various shear thinning fluids may be the critical factor responsible for different responses of the nematodes. Also, recent numerical and experimental studies on the swimming behavior of swimmers in complex fluids indicated that the viscoelastic property could either enhance or retard the swimming speed and locomotive efficiency of undulatory swimmers depending on either their body geometries and dynamic behaviors or fluid properties.<sup>19,20,24,37</sup> In a shear thinning PS colloidal suspension, we have observed the alteration in the stroke form of the nematode that must occur through the combinatorial effects of adaptively increased muscle power in viscous media and a drastic change in the apparent shear viscosity. As a result, with larger muscular power generated in the fully contracted state, the nematodes effectively move in the media with similar apparent viscosity compared to that in water. Our experimental results suggest a new plausible mechanism for the improvement in motion for many organisms living in non-Newtonian complex fluids where a shear thinning phenomenon in the medium could induce the changes in the neuromuscular power that varies both spatially and temporally along the nematode's body to swim against the imposed drag most effectively. In other words, the alterations in the physical properties of the surrounding environment could lead to the adaptive changes in animal locomotion in a manner that it would enhance their motile efficiency.

## Acknowledgements

We thank C. H. Choi for supporting the PS colloidal particles, J. N. Wilking for technical assistance with rheological measurements, and C. S. Lee and L. Mahadevan for insightful discussion. This work was supported by the National Research Foundation (NRF) grant 2013R1A1A2012420 (J. Park) and 2010-0016886 (D. Kim and J. Shin). The work at Harvard was supported by the NSF (DMR-1310266) and the Harvard MRSEC (DMR-0820484).

## References

- 1 L. Fauci and R. Dillon, *Annu. Rev. Fluid Mech.*, 2006, **38**, 371.
- 2 S. Suarez and A. Pacey, *Hum. Reprod Update*, 2006, **12**, 23.
- 3 E. Lauga and T. R. Powers, *Rep. Prog. Phys.*, 2009, **72**, 096601.
- 4 J. G. White, E. Southgate, J. N. Thomson and S. Brenner, *Philos. Trans. Roy. Soc., B*, 1986, **314**, 1.
- 5 Y. Magariyama and S. Kudo, *Biophys. J.*, 2002, **83**, 733.
- 6 E. Lauga, *Soft Matter*, 2011, **7**, 3060.
- 7 P. Kanehl and T. Ishikawa, *Phys. Rev. E: Stat. Phys., Plasmas, Fluids, Relat. Interdiscip. Top.*, 2014, **89**, 042704.
- 8 S. S. Sharpe, S. A. Koehler, R. M. Kuckuk, M. Serrano, P. A. Vela, J. Mendelson and D. I. Goldman, *J. Exp. Biol.*, 2015, **218**, 440.
- 9 J. Gray and G. J. Hancock, *J. Exp. Biol.*, 1955, **32**, 802.
- 10 S. Jung, S. Lee and A. Samuel, *Chaos*, 2008, **18**, 041106.
- 11 S. Jung, *Phys. Fluids*, 2010, **22**, 031903.
- 12 G. Juarez, K. Lu, J. Sznitman and P. E. Arratia, *Europhys. Lett.*, 2010, **92**, 44002.
- 13 B. Han, D. Kim, U. H. Ko and J. H. Shin, *Lab Chip*, 2012, **12**, 4128.
- 14 S. Gart, D. Vella and S. Jung, *Soft Matter*, 2011, **7**, 2444.
- 15 S. S. Suarez and X. Dai, *Biol. Reprod.*, 1992, **46**, 686.
- 16 D. J. Smith, E. A. Gaffney, H. Gadêlha, N. Kapur and J. C. Kirkman-Brown, *Cell. Motil. Cytoskeleton*, 2009, **66**, 220.
- 17 R. D. Maladen, Y. Ding, C. Li and D. I. Goldman, *Science*, 2009, **325**, 314.
- 18 Y. D. S. S. Sharpe, C. Li and D. I. Goldman, *J. Exp. Biol.*, 2013, **216**, 260.
- 19 S. E. Spagnolie, B. Liu and T. R. Powers, *Phys. Rev. Lett.*, 2013, **111**, 068101.
- 20 M. Dasgupta, B. Liu, H. C. Fu, M. Berhanu, K. S. Breuer, T. R. Powers and A. Kudrolli, *Phys. Rev. E: Stat. Phys., Plasmas, Fluids, Relat. Interdiscip. Top.*, 2013, **87**, 013015.
- 21 S. Nakamura, Y. Adachi, T. Goto and Y. Magariyama, *Biophys. J.*, 2006, **90**, 3019.
- 22 E. E. Riley and E. Lauga, *Europhys. Lett.*, 2014, **108**, 34003.
- 23 E. E. Riley and E. Lauga, *J. Theor. Biol.*, 2015, **382**, 345.
- 24 B. Thomases and R. D. Guy, *Phys. Rev. Lett.*, 2014, **113**, 098102.
- 25 A. M. Leshansky, *Phys. Rev. E: Stat. Phys., Plasmas, Fluids, Relat. Interdiscip. Top.*, 2009, **80**, 051911.
- 26 H. C. Fu, V. B. Shenoy and T. R. Powers, *Europhys. Lett.*, 2010, **91**, 24002.
- 27 D. A. Gagnon, X. N. Shen and P. E. Arratia, *Europhys. Lett.*, 2013, **104**, 14004.
- 28 J. R. Vélez-Cordero and E. Lauga, *J. Non-Newton Fluid Mech.*, 2013, **199**, 37.
- 29 T. D. Montenegro-Johnson, D. J. Smith and D. Loghin, *Phys. Fluids*, 2013, **25**, 081903.
- 30 G. Li and A. M. Ardekani, *J. Fluid Mech.*, 2015, **785**, R4.
- 31 V. A. Martinez, J. Schwarz-Linek, M. Reufer, L. G. Wilson, A. N. Morozov and W. C. K. Poon, *Proc. Natl. Acad. Sci. U. S. A.*, 2014, **111**, 17771.
- 32 X. N. Shen and P. E. Arratia, *Phys. Rev. Lett.*, 2011, **106**, 208101.
- 33 D. A. Gagnon, N. C. Keim and P. E. Arratia, *J. Fluid Mech.*, 2014, **758**, R3.
- 34 S. Brenner, *Genetics*, 1974, **77**, 71.
- 35 N. J. Wagner and J. F. Brady, *Phys. Today*, 2009, 27.
- 36 X. Cheng, J. H. McCoy, J. N. Israelachvili and I. Cohen, *Science*, 2011, **333**, 1276.
- 37 J. Teran, L. Fauci and M. Shelley, *Phys. Rev. Lett.*, 2010, **104**, 038101.
- 38 J. Sznitman, X. Shen, R. Sznitman and P. E. Arratia, *Phys. Fluids*, 2010, **22**, 121901.
- 39 J. Korta, D. A. Clark, L. M. C. V. Gabel and A. D. T. Samuel, *J. Exp. Biol.*, 2007, **210**, 2383.
- 40 C. Fang-Yen, M. Wyart, J. Xie, R. Kawai, T. Kodger, Q. W. S. Chen and A. D. T. Samuel, *Proc. Natl. Acad. Sci. U. S. A.*, 2010, **47**, 20323.
- 41 J. Sznitman, X. Shen, P. K. Purohit and P. E. Arratia, *Exp. Mech.*, 2010, **50**, 1303.
- 42 X. N. Shen, J. Sznitman, P. Krajacic, T. Lamitina and P. E. Arratia, *Biophys. J.*, 2012, **102**, 2772.
- 43 Y. Man and E. Lauga, *Phys. Rev. E: Stat. Phys., Plasmas, Fluids, Relat. Interdiscip. Top.*, 2015, **92**, 023004.
- 44 D. M. Kalyon, *J. Rheol.*, 2005, **49**, 621.